

## Suppression of Water Formation over Stepped Pt(335) by Au

D. C. Skelton,<sup>†,§,⊥</sup> R. G. Tobin,<sup>‡,†</sup> Galen B. Fisher,<sup>§,†,||</sup> David K. Lambert,<sup>\*,§,†,||</sup> and Craig L. DiMaggio<sup>§,||</sup>

Center for Sensor Materials, Michigan State University, East Lansing, Michigan 48824-1116, Department of Physics and Astronomy, Tufts University, Medford, Massachusetts 02155, and General Motors Research and Development Center, Warren, Michigan 48090-9055

Received: May 19, 1999; In Final Form: November 20, 1999

A partial monolayer of Au strongly modifies the kinetics of water adsorption and formation on the stepped Pt(335) surface. The effects are more than passivation. With a Au coverage of 0.7 ML as measured by Auger spectroscopy, saturation H and O adsorption are only 15% and 8.5%, respectively, of their values on bare Pt. Adsorption at step sites is nearly eliminated. Water formation is reduced to 5% of its bare Pt value: one-sixth of what would be expected if each Au atom blocked one site. Water formation on Pt has multiple reaction pathways. The partial Au layer eliminates only the low-temperature pathway. The H recombination temperature is reduced relative to bare Pt, so H recombination competes with water formation and reduces its efficiency. The partial Au layer also changes the desorption spectrum of water. At low water coverage, there is a single desorption peak, intermediate in temperature between those seen on Pt and Au.

## 1. Introduction

We have used temperature-programmed reaction (TPR) measurements to study the water formation reaction ( $2\text{H}_2 + \text{O}_2 \rightarrow 2\text{H}_2\text{O}$ ) on a stepped Pt surface partially covered by Au. This reaction has been widely studied.<sup>1–22</sup> In the context of automotive technology it occurs in catalytic converters, fuel cells, and electrochemical air-to-fuel ratio sensors. Adding Au to the Pt electrodes of zirconia-based sensors has been shown to increase sensitivity to  $\text{H}_2$  and other oxidizable gases,<sup>23,24</sup> and such modifications could eventually lead to on-board detection of catalytic converter malfunction.

Despite the apparent simplicity of the water formation reaction, its microscopic mechanisms on Pt have proved difficult to establish. It is clear that the reactants are atomically adsorbed H and O.<sup>2,3,5</sup> The reaction proceeds through a hydroxyl (OH) intermediate,<sup>9,11,19</sup> so the initial steps are dissociative adsorption of both O and H and hydroxyl formation ( $\text{H}_a + \text{O}_a \rightarrow \text{OH}_a$ ). The final water formation step could occur through addition of hydrogen ( $\text{H}_a + \text{OH}_a \rightarrow \text{H}_2\text{O}_a$ ), disproportionation ( $2\text{OH}_a \rightarrow \text{H}_2\text{O}_a + \text{O}_a$ ),<sup>9,11,19</sup> or via a peroxy-like intermediate ( $\text{H}_2\text{O}_2 \rightarrow \text{H}_2\text{O}_a + \text{O}_a$ ).<sup>17,21</sup> It is likely that the dominant process depends on the reaction condition. Verheij and co-workers have proposed that the reaction occurs only at special “reaction sites” present in concentrations  $\sim 10^{-6}$  on a well-prepared Pt(111) surface and that the remainder of the surface is catalytically inert.<sup>13,17,21</sup> They have also suggested an autocatalytic process for H transport below the  $\text{H}_2\text{O}$  desorption temperature.<sup>17,21</sup> Hellsing and co-workers, on the other hand, favor a model in which the reaction occurs homogeneously over the surface.<sup>10,15,19,20</sup> Recently,

Völkening et al. have also proposed an autocatalytic reaction at low temperatures, but for hydroxyl formation rather than H transport.<sup>22</sup>

The reaction occurs at temperatures as low as 120 K. Exposure of an O precovered surface to gas-phase  $\text{H}_2$  at 120 K reacts all of the O to  $\text{H}_2\text{O}$ , which desorbs at 180 K.<sup>3,7</sup> When a Pt surface with both  $\text{O}_a$  and  $\text{H}_a$  is heated in a temperature programmed reaction (TPR) experiment, however, the reactants are not all consumed below 180 K. In addition to the “desorption-limited” water peak at 180 K, from water formed at lower temperature, two or more “reaction-limited” peaks are observed between 200 and 300 K, indicating the presence of additional reaction channels with a higher activation energy.<sup>3,16</sup> On the partially Au-covered surface only these higher temperature channels are active.

Hydrogen adsorption on Pt is also controversial. Several authors have concluded that  $\text{H}_2$  dissociates even on flat Pt surfaces at temperatures as low as 90 K,<sup>3,16,25,26</sup> and its sticking coefficient is enhanced only modestly by the presence of steps.<sup>16,26,27</sup> Other authors have concluded that  $\text{H}_2$  dissociation occurs exclusively at the defect sites.<sup>28,29</sup> Oxygen dissociation also occurs more readily at steps, although it does occur on nearly ideal (111) surfaces.<sup>30,31</sup> As a result, stepped surfaces display enhanced catalytic activity for water formation at low O coverage, when  $\text{O}_2$  adsorption is rate limiting.<sup>16</sup> Very small concentrations ( $< 0.02$ ) of defects can dramatically increase the reaction rate.<sup>13</sup> Under other conditions, steps may slow the reaction by trapping H or OH in tightly bound states.<sup>5,16</sup> In reactions over dispersed Pt catalysts, the reaction rate increases as particle size decreases.<sup>6</sup>

In view of the importance of surface structure, we have examined the reaction on a highly stepped Pt surface, Pt(335), or Pt(s)[4(111)  $\times$  (100)] in step-terrace notation. This surface consists ideally of (111)-oriented terraces, four atoms wide, separated by monatomic-height steps of (100) orientation.

Pure Au neither adsorbs nor dissociates  $\text{H}_2$  or  $\text{O}_2$ , and is thus inert for water formation.<sup>32–37</sup> We find the same behavior when

\* Corresponding author. E-mail: David.K.Lambert@delphiauto.com.

<sup>†</sup> Michigan State University.

<sup>‡</sup> Tufts University.

<sup>§</sup> General Motors Research and Development Center.

<sup>||</sup> Present address: Delphi Central Research and Development, Warren, MI 48090-9055.

<sup>⊥</sup> Present address: Kimball Physics, Wilton, NH 03086.

the Pt(335) surface is fully covered by a monolayer (ML) of Au. Often, a metallic monolayer on a dissimilar metal exhibits electronic and chemical properties distinct from either bulk material.<sup>38–44</sup> This is what we observe with 0.7 ML of Au on Pt(335).

## 2. Experimental Section

The experiments were carried out in an ultrahigh vacuum chamber at the General Motors Research and Development Center. The chamber houses an Auger electron spectrometer, quadrupole mass spectrometer, four-screen front-view low-energy electron diffraction (LEED) optics, high resolution electron energy loss spectrometer (HREELS), and four parallel-array dosers, and has a base pressure of  $2 \times 10^{-11}$  Torr. Details of the preparation, cleaning, characterization, and dosing procedures are given in ref 45, and references therein.

Gold was evaporated in situ from a well-outgassed filament. The gold coverage was determined with Auger spectroscopy by comparison with the calibration curves of Sachtleir et al.<sup>46,47</sup> The calibration is supported by our observation that at an Au coverage of 1.1 ML, as determined from Auger spectroscopy, the surface was inactive for the adsorption of oxygen and hydrogen and displayed no LEED pattern. Scanning tunneling micrographs of our sample, with a nominal gold coverage of 0.7 ML, measured in air, revealed Au structures approximately 2 atomic layers high and  $\sim 30$  nm in diameter, covering about 30% of the surface. Adsorption experiments showed that the step sites were passivated by Au even in the apparently gold-free areas.<sup>45</sup>

The LEED pattern from the 0.7 ML Au/Pt surface was identical to the pattern from bare Pt(335). Since no additional spots were detected from the gold layer, the gold layer is assumed to be disordered.

The adsorption and reaction data presented in this work were collected using temperature programmed desorption with a heating rate of 10 K/s. Oxygen and hydrogen coverages were calculated from the integrated areas under the desorption spectra and are presented as a percent of the saturation coverage on a particular surface. The uncertainty in the coverages is  $\pm 10\%$ .

## 3. Thermal Desorption of Individual Adsorbates

**3.1. Hydrogen and Oxygen. Bare Pt(335).** The desorption of H<sub>2</sub> and O<sub>2</sub> from Pt(335) is well documented.<sup>27,31,45,48–50</sup> Hydrogen adsorbs dissociatively down to 90 K, and has two desorption features: recombinative desorption from the terraces at 315 K at low coverage, shifting down to 280 K at saturation, and recombinative desorption from the steps at 395 K. The step sites fill to completion before the terrace begins to fill. Desorption of H<sub>2</sub> from Pt(335) is shown in Figure 1a.

Oxygen desorption from Pt(335) has three main features: molecular desorption at 120 K, atomic recombination from the terraces at 750 K, and atomic recombination from the steps at 850 K. Also, a peak at 210 K is attributed to molecular desorption from the steps.<sup>31</sup> These features are shown in Figure 2a.

**1.1 ML Au/Pt(335).** This surface neither adsorbs nor dissociates H<sub>2</sub> or O<sub>2</sub>. The desorption traces are shown in Figure 1c and Figure 2c, respectively, and are featureless. The inability of Au to dissociate H<sub>2</sub> is understood theoretically.<sup>51</sup>

**0.7 ML Au/Pt(335).** Our previous observations of CO and O<sub>2</sub> on this surface are consistent with a model that has both Au-covered regions and Pt regions that are largely free of Au.<sup>45</sup>

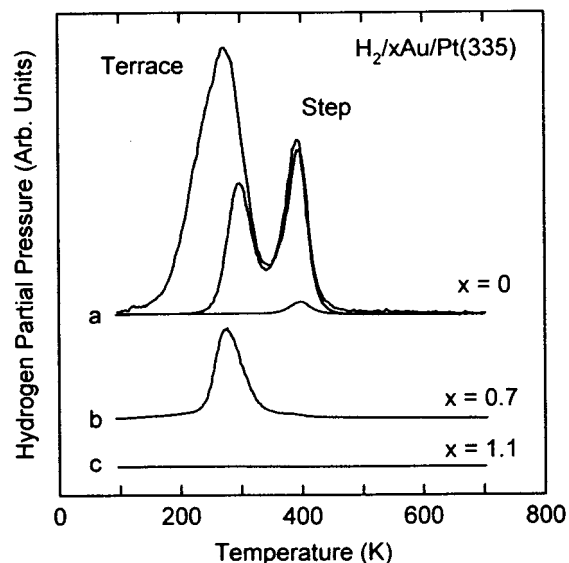


**Figure 1.** Desorption of H<sub>2</sub> from Pt(335), bare and at two Au coverages: 0.7 and 1.1 ML. On bare Pt(335) three H-coverages are shown: 1%, 44%, and saturation. The same scale is used for all curves.

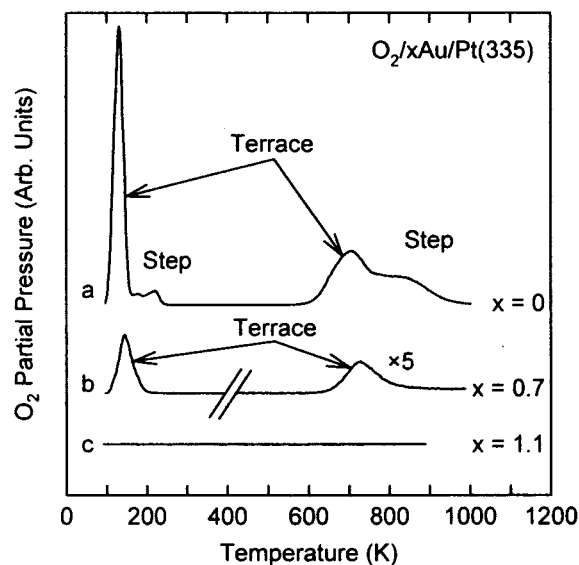


**Figure 2.** Desorption of O<sub>2</sub> from Pt(335), bare and at two Au coverages: 0.7 and 1.1 ML. Each has been dosed with O<sub>2</sub> to saturation. The same scale is used for all curves.

Within the Pt regions the step sites are occupied by Au, as evidenced by the suppression of step-site adsorption for both O and CO.

Desorption of O<sub>2</sub>, shown in Figure 2b, is discussed in ref 45. Two major features are retained from Pt(335): desorption of molecular O<sub>2</sub> near 120 K and recombination of terrace atomic O at approximately 750 K. The maximum oxygen coverage is only 8.5% of the coverage on bare Pt(335), even though at least 30% of the Pt surface remains exposed.<sup>52</sup> No peak attributable to O at step sites is discernible: step site O coverage is at most 6% of its value on Pt(335). To explain this low coverage, we have proposed a model in which O<sub>2</sub> dissociates only at special sites near the Pt–Au boundaries.<sup>45</sup> The hot O atoms released by dissociation are known<sup>53</sup> to move 2 to 4 lattice spacings before becoming immobile, at temperatures  $< 300$  K.<sup>17,31,54</sup> This would limit O to a small fraction of the exposed Pt surface area. Other explanations can certainly be imagined, however, and this mechanism cannot explain the low hydrogen coverage on the

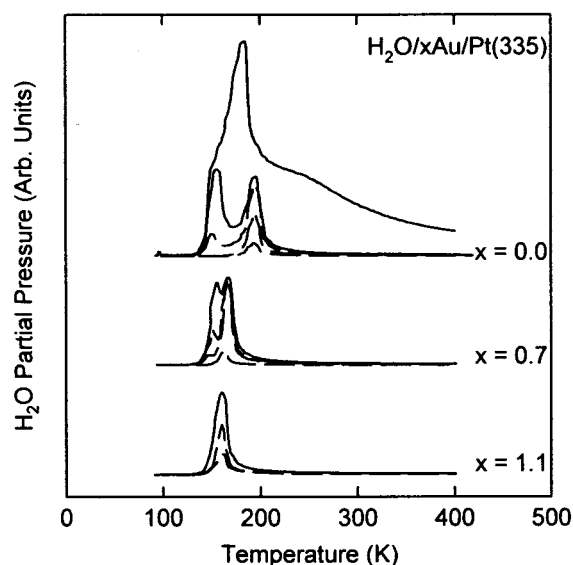


**Figure 3.** Desorption of water from Pt(335), bare and at two Au coverages. The evolution of the desorption spectrum with water coverage is shown for all three surfaces. The same scale is used for all curves.

Au-covered surface, because H atoms are mobile on Pt even at low temperatures.

Although  $O_2$  will not dissociate on pure Au, atomic O can be adsorbed on Au by dosing with either O atoms or with molecules containing weakly bound O.<sup>34,55–57</sup> Atomic O on Au is evidenced by an  $O_2$  recombination peak at 500 to 600 K.<sup>34,57</sup> No such peak was seen from 0.7 ML Au/Pt(335), suggesting that O is only on the Pt.

The desorption of  $H_2$  from the 0.7 ML Au/Pt(335) surface is shown in Figure 1b. The Au has two effects: it reduces total  $H_2$  desorption to 15% of that from bare Pt(335) and it reduces the area of the peak at 400 K (from step site H) to 3% of that from bare Pt(335). A peak from H on Pt terraces remains. The blockage of step sites with Au is not complete, however, since there is a vestigial peak from H at step sites. It is not clear why the saturation H coverage is smaller than the fraction of Pt surface exposed. The fact that Au suppresses O adsorption more strongly than H adsorption may be because O has a stronger preference for step sites. At saturation oxygen coverage on the bare surface, the fractional occupation of step sites is probably higher than that of terrace sites, whereas for hydrogen the occupation of both step and terrace sites is probably near unity. As a result the proportion of oxygen on step sites is higher than for hydrogen, and oxygen adsorption is more strongly affected by the blockage of the steps by gold.

Like O, H can be adsorbed on Au by predissociation in the gas phase. Adsorbed atomic H is characterized by recombinative desorption between 150 and 250 K.<sup>33–35,37</sup> The absence of desorption in that region in Figure 1b suggests that no H adsorbs on the Au-covered regions of the 0.7 ML Au/Pt(335) surface.

**3.2. Water.** The thermal desorption traces of  $CO$ ,  $O_2$ , and  $H_2$  from 0.7 ML Au/Pt(335) all show features characteristic of adsorption on bare Pt (although  $CO$  shows additional peaks<sup>45</sup>). The desorption of water, shown in Figure 3, does not follow this trend.

The two peaks that are observed for water desorption from both bare Pt(335) and 0.7 ML Au/Pt(335) are typical of water desorption from transition metals.<sup>58,59</sup> For both, as the water coverage increases, the higher-temperature feature (195 K for bare Pt, 165 K for Pt with 0.7 ML Au) grows in first. It is attributed to the first layer of chemisorbed water, the inner half

of a bilayer.<sup>60–63</sup> The first layer is bonded directly to the surface. The outer half of the bilayer is hydrogen-bonded to the first layer.<sup>62,63</sup> The lower temperature peak (155 K for both surfaces) appears after saturation of the first layer peak, and with increasing coverage grows to equal its intensity; we attribute the 155 K feature to physisorbed water (ice) growing on top of the first layer.<sup>60–63</sup> With greater exposure to water, the 155 K feature grows, broadens, and shifts to higher temperature. After several layers it assumes the form shown as the highest coverage curve for Pt(335) in Figure 3, regardless of the substrate. This behavior is typical of ice multilayers and has been observed on many metals.<sup>58,59</sup> The third curve in each sequence was measured at the completion of the bilayer – the exposure at which the 155 K ice peak reached maximum intensity before beginning to shift upward in temperature.

With 1.1 ML Au/Pt(335), the higher temperature feature is absent. At low coverage, a single asymmetric peak at 160 K is seen. At higher coverage it evolves to the multilayer form shown in the top trace. This is similar to water adsorption on Au(111).<sup>64</sup>

It is difficult to associate the water desorption peaks from the 0.7 ML Au/Pt(335) surface with adsorption on Pt or Au. The integrated areas of the first- and second-layer peaks on the 0.7 ML Au/Pt(335) surface are  $70 \pm 10\%$  of the areas of the corresponding peaks on bare Pt(335). While at least 30% of the Pt area is exposed, it is unlikely that 70% of the Pt is exposed, given the Auger measurements and the saturation coverages of the other molecules in this study. This suggests that water also adsorbs on the Au. If so, we would have expected distinct first-layer peaks from the two regions, as for  $CO$ .<sup>45</sup> Perhaps the water is sufficiently mobile<sup>57</sup> that all of the desorption occurs from the most weakly bound state – probably on the Au – even though the water is initially adsorbed on both metals. However, this does not explain why two desorption peaks are seen at higher water coverages on 0.7 ML Au/Pt(335), while only one is observed for adsorption on Au.<sup>64,65</sup>

For the purpose of examining the water formation reaction, the central point is that water desorption is complete by 200 K, regardless of Au coverage.

#### 4. Water Formation

In previous experiments on Pt(111), two distinct channels have been seen for water formation: a low-temperature pathway, in which the water remains on the surface until the water desorption temperature ( $\sim 180$  K) is reached, and one or more higher-temperature pathways where reaction occurs above the water desorption temperature and the water desorbs shortly after formation.<sup>2,3,16,18,21</sup> If the O-precovered surface is exposed to gas phase  $H_2$  above 120 K, however, or repeatedly dosed with  $H_2$  at low temperature ( $< 120$  K) and annealed to 135 K, all of the O can be incorporated into water below 135 K.<sup>3,7</sup> Therefore all of the O is accessible to the low-temperature reaction channel, and the presence of the higher-temperature TPR peaks is due to kinetic factors.

There is evidence that different reaction mechanisms dominate water formation in the low- and high-temperature regions. The nature of the mechanisms remains in dispute and may depend not only on temperature but also on reactant coverages and even prior history.<sup>2</sup> A number of studies have suggested that the dominant pathway at high temperature is H addition to  $OH$ ,<sup>5,10,14,17</sup> while disproportionation, either from  $2OH$  or from an  $H_2O_2$  intermediate, may be more important at low temperature.<sup>5,17,19,21</sup> On Pd surfaces, disproportionation has been shown to be dominant at low temperature.<sup>65</sup> On Pt, however, the low-temperature mechanism remains unclear. The recent work of



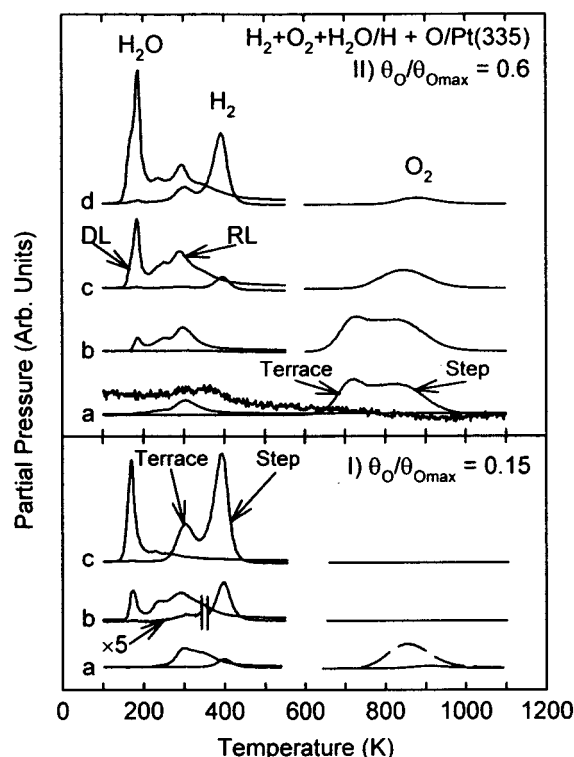


**Figure 4.** Desorption of water,  $O_2$ , and  $H_2$  from Pt(335) prepared with atomic O and H. The labels DL and RL in part (II) point to the desorption-limited and reaction-limited water desorption peaks, respectively. Initial O coverage as a fraction of saturation is listed on the figure. The initial coverages of H for part (I) are: (a) 15%, (b) 45%, and (c) 100% of saturation. The dashed line in the oxygen region of curve (a) in part (I) shows  $O_2$  desorption for the same O coverage without H. Terrace desorption in curve (b) part (I) has been expanded by a factor of 5. The initial H coverages in part (II) are: (a) 7%, (b) 15%, (c) 40%, and (d) 75%. The desorption of  $H_2$  in curve (a) part (II) is expanded by a factor of 10 to show that  $H_2$  desorbs from the terraces even at low H coverages when O fills the step sites. The curves of part (I) clearly show that terrace H is necessary for the desorption-limited peak.

Völkening et al. suggests that the presence of adsorbed water at low temperature facilitates hydroxyl formation and thereby autocatalyzes the reaction.<sup>22</sup> Our results support the view that the low- and high-temperature reaction mechanisms are different.

In our TPR experiments the sample was initially exposed to  $O_2$  at 90 K, then flashed to 300 K to desorb and dissociate the adsorbed  $O_2$ , leaving a partial coverage of O. The sample was then exposed to  $H_2$  at 90 K and heated at 10 K/s while desorption of  $H_2$ ,  $O_2$ , and  $H_2O$  were monitored. All coverages are expressed as a fraction of the maximum coverage achievable on the corresponding surface in the absence of coadsorbates. The O and H coverages are  $\theta_O$  and  $\theta_H$ , respectively.

**Bare Pt(335).** Figure 4 shows TPR data at two  $O_2$  doses ( $\theta_O \sim 15\%$  and  $60\%$  of saturation) and varying  $H_2$  doses. At the higher  $O_2$  dose, four water desorption features are seen: a peak at 350 K, which is dominant at  $5\% \theta_H$  and  $15\% \theta_O$  (not shown); a peak at 300 K, which grows with  $\theta_H$ ; a peak at 220 K, which becomes prominent only after the desorption-limited  $H_2O$  peak has appeared; and the desorption-limited peak at 180 K, which is evident even at the lowest  $\theta_H$  with  $30\% \theta_O$  (not shown). The peak at 350 K is more easily seen at lower  $O_2$  doses in part (I) curve (a) of Figure 4.

The desorption-limited peak contains a larger proportion of the water in these spectra than in comparable traces from Pt-

(111).<sup>3,16</sup> Moreover, as we show below, it is absent on the partially Au covered surface, where Au blocks the step sites. These observations suggest that the low-temperature reaction channel involves step sites. Other experiments, however, indicate that step H is available for reaction only at higher temperatures.<sup>5,16</sup>

The data in Figure 4 show that only *terrace* H participates in the low-temperature ( $<180$  K) reaction process. At the lower  $\theta_O$  shown in part (I) of Figure 4, O occupies only step sites, but does not fill them. At low  $\theta_H$  we then observe  $H_2$  desorption from the step sites without measurable desorption from the terrace sites. Under these conditions, with no terrace H present, only the reaction-limited peaks (above 200 K) appear in the water desorption shown in part (I) curve (a) of Figure 4. The appearance of the desorption-limited (180 K) peak in the water curve tends to coincide with the appearance of  $H_2$  desorption from terrace sites in part (I) curve (b) of Figure 4.

These observations lead to the conclusion that the low-temperature reaction channel requires H at terrace sites. The step H, which is more tightly bound, reacts only at temperatures above 200 K. We cannot conclude, of course, that terrace H reacts *only* at low temperature; it may also participate in the higher-temperature reaction channels.

**0.7 ML Au/Pt(335).** Partially covering the Pt surface with Au drastically reduces its catalytic activity. The maximum amount of  $H_2O$  produced in a TPR experiment is only 5% of the amount produced on bare Pt(335). The smaller quantity of reactants available (8.5% of O and 15% of H) cannot fully account for the change. There is a reduced reaction probability for H. (Since O leaves only at much higher temperatures, it is the behavior of the H that determines the reaction efficiency: on Pt(111) 100% of the O reacts if sufficient H is available.<sup>16</sup>)

Figure 5 shows a series of TPR traces for varying  $\theta_H$  at a fixed  $O_2$  dose. Three changes from the bare Pt surface are seen. First, hydrogen desorption from step sites is eliminated under these dosing conditions. Second, the peak desorption temperature for terrace H is shifted down by 20 K, to coincide with the main water production peak. Finally and most strikingly, no water desorption is seen below 200 K. Since we know from Figure 3 that any adsorbed water on the surface would desorb below 200 K, the absence of a peak indicates that the *lowest temperature reaction channel on the bare surface is deactivated by the partial Au overlayer*.

We performed a titration experiment to determine the extent of the deactivation. The surface was prepared with  $O_a$  as described previously, and then exposed to  $1 \times 10^{-7}$  Torr  $H_2$  at several temperatures between 90 and 135 K, with exposure times ranging from 1 to 20 min. Water desorption was then monitored as the sample was heated, and no peak below 200 K was observed. The rate of the lowest-temperature channel is reduced by at least 70 times on the partially Au-covered surface compared to the bare surface.

On bare Pt, direct desorption of  $H_2$  has relatively little influence on the availability of  $H_a$  to form water.<sup>5,16,18</sup> There is an efficient low-temperature reaction channel for terrace H, and the desorption temperatures of both terrace H and step H are higher than the water TPR peaks. Provided that ample  $O_a$  is available, most of the  $H_a$  will react. On Pt(111), the reaction probability for (terrace) H was found to be  $>90\%$ .<sup>16</sup> Other measurements also indicate that  $H_2$  desorption does not compete strongly with water formation on Pt(111).<sup>5,18</sup> This is illustrated by the filled symbols in Figure 6, which displays the probability that an adsorbed H atom will leave the surface as part of a water

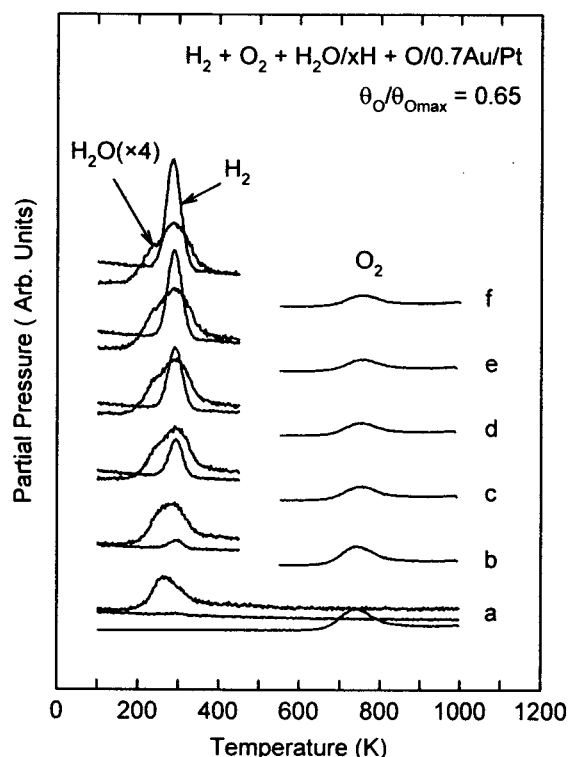


**Figure 5.** Desorption of water,  $O_2$ , and  $H_2$  from 0.7 ML Au/Pt(335). Initial O coverage is listed on the figure and the H coverages from curves (a) to (f) are: 4%, 7%, 13%, 21%, 28%, and 36% of saturation. In comparison to Figure 4, the desorption curves for  $H_2$ ,  $O_2$ , and  $H_2O$  are magnified here by factors of 5, 2.5, and 10, respectively.

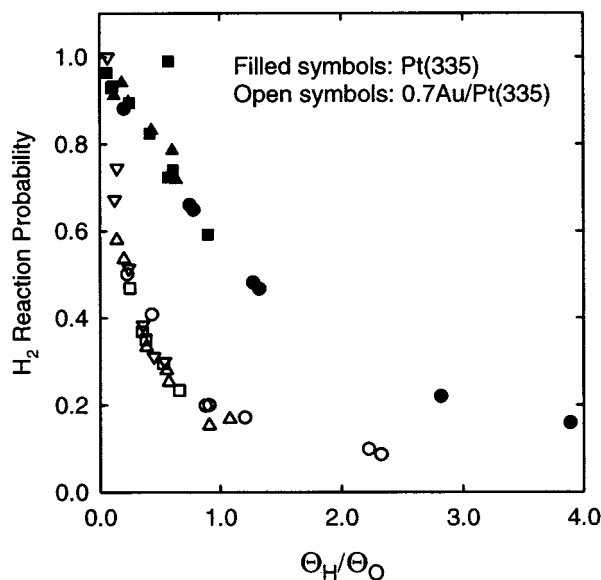


**Figure 6.** Reaction probabilities per  $H_2$  molecule on Pt(335) (filled symbols) and 0.7 ML Au/Pt(335) (open symbols), as a function of the hydrogen-oxygen ratio  $\theta_H/\theta_O$ , for various initial oxygen coverages. For bare Pt the approximate oxygen coverages were 0.15, 0.4, and 0.5; for Au/Pt they were 0.2, 0.3, 0.5, and 0.6, in each case relative to the saturation coverage on the same surface. Reaction probabilities were calculated as the integrated area of water desorption divided by the integrated area of ( $H_2 + H_2O$ ) desorption.

molecule rather than as  $H_2$ , as a function of the ratio of adsorbed hydrogen to adsorbed oxygen  $\theta_H/\theta_O$ . The figure includes data for three initial oxygen doses representing coverages from 10% to 70% of saturation. The H reaction probability drops gradually from near unity as the relative availability of oxygen decreases; even at  $\theta_H/\theta_O = 4$  the reaction probability is nearly 20%. These

considerations become important when we look at the partially Au covered surface.

The greater competition between desorption and reaction on 0.7 ML Au/Pt(335) is reflected in the reaction probability, shown by the open symbols in Figure 6, which include data for four initial oxygen doses, representing coverages from 15% to 70% of saturation. The H reaction probability drops much more rapidly at low  $\theta_H$  than on bare Pt and appears to approach zero asymptotically. We can understand this behavior qualitatively: at temperatures near 300 K, a mobile  $H_a$  diffuses on the surface in an environment of O, OH, and H. If it encounters an OH or an H, it is likely to form  $H_2O$  or  $H_2$  and immediately desorb. The reaction probability therefore depends in part on the relative likelihood of encountering an OH rather than an H, and as  $\theta_H$  increases, that likelihood diminishes.

This model is further supported by the fact that, for both surfaces, the reaction probability data for different oxygen coverages fall on a single curve, indicating that  $\theta_H/\theta_O$  is the key parameter, as expected for a statistical process. The presence of the gold simply shifts the odds in favor of desorption rather than reaction.

## 5. Conclusions

The microscopic mechanism of even a relatively simple reaction on a surface can be subtle. Recent calculations, for example, suggest that the crucial step in CO oxidation on Pt-(111) involves a coordinated *pas de deux* between the reactants over a particular area of the unit cell.<sup>67</sup> The water formation reaction is even more intricate. The reaction rate is not a unique function of the reactant coverages, but depends on the initial arrangement of the O atoms,<sup>2</sup> and surface modifications too slight to be detected by standard methods significantly change the reaction rate.<sup>13</sup> Special sites of unknown character and extreme rarity may dominate the reaction.<sup>13,17,21</sup> Anything that modifies the geometrical or electronic structure of the surface is likely to have a large, if currently unpredictable, effect on the reaction kinetics.

The experiments presented here illustrate this point. Based on adsorption measurements, it was expected that the partially Au covered surface would accommodate less O and H, and therefore produce less water. Processes involving step species would be strongly suppressed. Completely unexpected was the elimination of the low-temperature reaction process, which involves terrace species. The catalytic activity of the surface is reduced by at least a factor of 6 below what we would expect from Au simply blocking Pt sites.

There is considerable disagreement regarding the mechanism of the low-temperature water formation reaction. Verheij et al. postulate that both the low- and high-temperature reactions occur at special reaction sites.<sup>13,17,21</sup> Because O is immobile below 200 K, they propose a low-temperature mechanism involving disproportionation of an  $H_2O_2$  intermediate and H transport from the "reaction front" to the reaction site via  $H_2O_2$ .<sup>17,21</sup> Helling and co-workers dispute the need for special sites, but concur that disproportionation is likely to dominate H addition at low temperature.<sup>15,19</sup> Anton and Cadogan, on the other hand, find disproportionation to be a minor pathway with a higher activation energy than H addition.<sup>14</sup> The scanning tunneling images of Völkening et al., with  $H_2$  provided continuously to the O-precovered surface, clearly show a reaction front separating oxygen-covered and water-covered regions several hundred Å in extent.<sup>22</sup>

Our experiments support the idea that different mechanisms dominate at low and high temperatures. A partial monolayer of

Au effectively eliminates the low-temperature process, perhaps by inhibiting the formation of a 2OH or H<sub>2</sub>O<sub>2</sub> intermediate, or perhaps by blocking or disrupting the progress of the reaction front. Its effect on the high-temperature process arises largely from a lower H-desorption temperature.

**Acknowledgment.** The scanning tunneling microscopy was performed by Baokang Bi at Michigan State University. This work was supported by the National Science Foundation under Grants DMR-9696233 and DMR-9400417 (MRSEC).

## References and Notes

- (1) Fisher, G. B.; Sexton, B. A. *Phys. Rev. Lett.* **1980**, *44*, 683.
- (2) Gland, J. L.; Fisher, G. B.; Kollin, E. B. *J. Catal.* **1982**, *77*, 263.
- (3) Fisher, G. B.; Gland, J. L.; Schmieg, S. J. *J. Vac. Sci. Technol.* **1982**, *20*, 518.
- (4) Norton, P. R. In *Chemical Physics of Solid Surface and Heterogeneous Catalysis*; King, D. A., Woodruff, D. P., Eds.; Elsevier: Amsterdam, 1982.
- (5) Gdowski, G. E.; Madix, R. J. *Surf. Sci.* **1982**, *119*, 184.
- (6) Nieuwenhuys, B. E. *Surf. Sci.* **1983**, *126*, 307.
- (7) Ogle, K. M.; White, J. M. *Surf. Sci.* **1984**, *139*, 43.
- (8) Mitchell, G. E.; Akhter, S.; White, J. M. *Surf. Sci.* **1986**, *166*, 283.
- (9) Mitchell, G. E.; White, J. M. *Chem. Phys. Lett.* **1987**, *135*, 84.
- (10) Hellsing, B.; Kasemo, B.; Ljungström, S.; Rosén, A.; Wahnström, T. *Surf. Sci.* **1987**, *189/190*, 851.
- (11) Germer, T. A.; Ho, W. *Chem. Phys. Lett.* **1989**, *163*, 449.
- (12) Verheij, L. K.; Hugenschmidt, M. B.; Colln, L.; Poelsema, B.; Comsa, G. *Chem. Phys. Lett.* **1990**, *166*, 523.
- (13) Verheij, L. K.; Hugenschmidt, M. B.; Poelsema, B.; Comsa, G. *Chem. Phys. Lett.* **1990**, *174*, 449.
- (14) Anton, A. B.; Cadogan, D. C. *Surf. Sci. Lett.* **1990**, *239*, L548.
- (15) Hellsing, B.; Kasemo, B.; Zhdanov, V. P. *J. Catal.* **1991**, *132*, 210.
- (16) Kwasniewski, V. J.; Schmidt, L. D. *J. Phys. Chem.* **1992**, *96*, 5931.
- (17) Verheij, L. K.; Freitag, M.; Hugenschmidt, M. B.; Kemp, I.; Poelsema, B.; Comsa, G. *Surf. Sci.* **1992**, *272*, 276.
- (18) Verheij, L. K.; Hugenschmidt, M. B. *Surf. Sci.* **1995**, *324*, 185.
- (19) Fridell, E.; Elg, A.-P.; Rosén, A.; Kasemo, B. *J. Chem. Phys.* **1995**, *102*, 5827.
- (20) Eisert, F.; Rosén, A. *Surf. Sci.* **1997**, *377–379*, 759.
- (21) Verheij, L. K. *Surf. Sci.* **1997**, *371*, 100.
- (22) Völkening, S.; Bedürftig, K.; Jacobi, K.; Wintterlin, J.; Ertl, G. *Phys. Rev. Lett.* **1999**, *83*, 2672.
- (23) Baier, G.; Schüle, V.; Vogel, A. *Appl. Phys. A* **1993**, *57*, 51.
- (24) Vogel, A.; Baier, G.; Schüle, V. *Sens. Actuators B* **1993**, *15–16*, 147.
- (25) Baró, A. M.; Ibach, H.; Bruchmann, H. D. *Surf. Sci.* **1979**, *88*, 384.
- (26) Christmann, K.; Ertl, G. *Surf. Sci.* **1976**, *60*, 365.
- (27) Baró, A. M.; Ibach, H. *Surf. Sci.* **1980**, *92*, 237.
- (28) Poelsema, B.; Comsa, G. *Scattering of Thermal Energy Atoms from Disordered Surfaces*; Springer Tracts in Modern Physics 115; Springer-Verlag: New York, 1989; pp 88–91.
- (29) Kaukonen, H.-P.; Nieminen, R. M. *Surf. Sci.* **1991**, *247*, 43.
- (30) Hopster, H.; Ibach, H.; Comsa, G. *J. Catal.* **1977**, *46*, 37.
- (31) Wang, H.; Tobin, R. G.; Lambert, D. K.; DiMaggio, C. L.; Fisher, G. B. *Surf. Sci.* **1997**, *372*, 267.
- (32) Trapnell, B. M. W. *Proc. R. Soc. London Ser. A* **1953**, *218*, 566.
- (33) Pritchard, J.; Tomkins, F. C. *Trans. Faraday Soc.* **1960**, *56*, 540.
- (34) Sault, A. G.; Madix, R. J.; Campbell, C. T. *Surf. Sci.* **1986**, *169*, 347.
- (35) Lisowski, E.; Stobiński, L.; Duś, R. *Surf. Sci.* **1987**, *188*, L735.
- (36) Ljungström, S.; Kasemo, B.; Rosén, A.; Wahnström, T.; Fridell, E. *Surf. Sci.* **1989**, *216*, 63.
- (37) Stobiński, L.; Duś, R. *Surf. Sci.* **1992**, *269/270*, 383.
- (38) Campbell, R. A.; Rodriguez, J. A.; Goodman, D. W. *Phys. Rev. B* **1992**, *46*, 7077.
- (39) Sellidj, A.; Koel, B. E. *Surf. Sci.* **1993**, *284*, 139.
- (40) Sellidj, A.; Koel, B. E. *Phys. Rev. B* **1994**, *49*, 8367.
- (41) Rodriguez, J. A.; Campbell, R. A.; Goodman, D. W. *Surf. Sci.* **1994**, *307–309*, 377 and references therein.
- (42) Maciejewski, P.; Wurth, W.; Köstmeier, S.; Pacchioni, G.; Röscher, N. *Surf. Sci.* **1995**, *330*, 156.
- (43) Schröder, U.; Linke, R.; Boo, J.-H.; Wandelt, K. *Surf. Sci.* **1996**, *357–358*, 873.
- (44) Marinkovic, N. S.; Wang, J. X.; Marinkovic, J. S.; Adzic, R. R. *J. Phys. Chem. B* **1999**, *103*, 139.
- (45) Skelton, D. C.; Tobin, R. G.; Lambert, D. K.; Fisher, G. B.; DiMaggio, C. L. *J. Phys. Chem. B* **1999**, *103*, 964.
- (46) Sachtler, J. W. A.; Van Hove, M. A.; Bibérian, J. P.; Somorjai, G. A. *Surf. Sci.* **1981**, *110*, 19.
- (47) Sachtler, J. W. A.; Somorjai, G. A. *J. Catal.* **1983**, *81*, 77.
- (48) Wang, H.; Tobin, R. G.; Lambert, D. K. *J. Chem. Phys.* **1994**, *101*, 4277.
- (49) Rar, A.; Matsushima, T. *Surf. Sci.* **1994**, *318*, 89.
- (50) Wang, H.; Tobin, R. G.; Lambert, D. K.; Fisher, G. B.; DiMaggio, C. L. *Surf. Sci.* **1995**, *330*, 173.
- (51) Hammer, B.; Nørskov, J. K. *Nature* **1995**, *376*, 238.
- (52) Reference 45 lists the O coverage ratio as 10%. The difference between that value and the value of 8.5% used in this work reflects the uncertainty in Au coverage. The value of 30% exposed Pt area is based on 0.7 ML Au coverage from Auger spectroscopy, and is a lower bound. If the Au forms clusters, more Pt is exposed.
- (53) Wintterlin, J.; Schuster, R.; Ertl, G. *Phys. Rev. Lett.* **1996**, *77*, 123.
- (54) Lewis, R.; Gomer, R. *Surf. Sci.* **1968**, *12*, 157.
- (55) Outka, D. A.; Madix, R. J. *Surf. Sci.* **1987**, *179*, 351.
- (56) Canning, N. D. S.; Outka, D.; Madix, R. J. *Surf. Sci.* **1984**, *141*, 240.
- (57) Holmes Parker, D.; Koel, B. E. *J. Vac. Sci. Technol. A* **1990**, *8*, 2585.
- (58) Thiel, P. A.; Madey, T. E. *Surf. Sci. Rep.* **1987**, *7*, 211.
- (59) Heras, J. M.; Viscido, L. *Catal. Rev. Sci. Eng.* **1988**, *30*, 281.
- (60) Fisher, G. B.; Gland, J. L. *Surf. Sci.* **1980**, *94*, 446.
- (61) Sexton, B. A. *Surf. Sci.* **1980**, *94*, 435.
- (62) Thiel, P. A.; Hoffmann, F. M.; Weinberg, W. H. *J. Chem. Phys.* **1981**, *75*, 5556.
- (63) Jo, S. K.; Kiss, J.; Polanco, J. A.; White, J. M. *Surf. Sci.* **1991**, *253*, 233.
- (64) Kay, B. D.; Lykke, K. R.; Creighton, J. R.; Ward, S. J. *J. Chem. Phys.* **1989**, *91*, 5120.
- (65) Heras, J. M.; Albano, E. V. *Z. Phys. Chem. (Wiesbaden)* **1982**, *129*, 11.
- (66) Nyberg, C.; Tengstål, C. G. *J. Chem. Phys.* **1984**, *80*, 3463.
- (67) Alavi, A.; Hu, P.; Deutsch, T.; Silvestrelli, P. L.; Hutter, J. *Phys. Rev. Lett.* **1998**, *80*, 3650.